Available online at www.sciencedirect.com

ScienceDirect

IFAC PapersOnLine 52-2 (2019) 25–29

Robust Controller versus Numerical Model Uncertainties for Stabilization of Navier-Stokes Equations ⋆

Peter Benner *,** **Jan Heiland** *,** **Steffen W. R. Werner** *

* *Max Planck Institute for Dynamics of Complex Technical Systems, Magdeburg, Germany*
(e-mail: {benner, heiland, werner}@mpi-magdeburg.mpg.de)
** *Department of Mathematics, Otto von Guericke University, Magdeburg, Germany*

Abstract: We consider the stabilization of incompressible fluid flow using linearized and spatially discretized models. In order to potentially work in applications, the designed controller must stabilize the discrete model with a robustness margin that covers linearization, discretization, and modeling errors. We expand on previous results that a linearization error in the infinite-dimensional model amounts to a coprime factor uncertainty and show that $\mathcal{H}_\infty$-robust controllers can compensate this in the discrete approximation. In numerical experiments, we quantify the robustness margins and show that the $\mathcal{H}_\infty$-robust controller, unlike the LQG-controller, is capable of stabilizing nonlinear incompressible Navier-Stokes equations with an inexact linearization.

Keywords: robust control, descriptor systems, parameter-varying systems, output feedback control, infinite-dimensional systems

1. INTRODUCTION

Linearization-based output feedback controllers for set-point stabilization of laminar flows have been successfully employed in simulations; see Benner and Heiland (2015). However, in applications, one desires *robust controllers* that can bridge the gaps between the approximation and the model (with a certain guarantee) and (hopefully) the model and reality. In linearization-based (flow) control there are several targets for robustness:

(1) domain of attraction – the controllers work if perturbations are small; see Raymond (2006) for theory,
(2) uncertainty in the linearization point; see Benner and Heiland (2016),
(3) approximation of the infinite-dimensional model by discretization and model reduction; see Benner and Heiland (2017).

In this paper, we resume the discussion of linearization uncertainties and robust controllers as started for infinite-dimensional linearized incompressible Navier-Stokes equations in Benner and Heiland (2016). We combine analytical results and confirm numerically that, for a given discretization, standard $\mathcal{H}_\infty$-control theory provides robust controllers that can compensate errors in the linearization.

The robustness margin of the controllers is measured in terms of maximally admissible deviations in coprime factorizations of the computed and the (hypothetical) exact transfer function. Also, the considered Galerkin discretizations of the infinite-dimensional system are known to converge in terms of coprime factors (see Morris (1994) for the general theory, Benner and Heiland (2017) for the extension to the incompressible Navier-Stokes equation and Badra (2006) for general estimates on the convergence of such approximations as well as results on uniform stabilizability). Thus, the robustness of the controllers similarly covers discretization and linearization errors so that the presented results, together with Benner and Heiland (2017), can be seen as a general approach to robust stabilization of infinite-dimensional systems by numerically approximated models.

In a previous work (Benner and Heiland (2016)) we have shown, that the linearized (infinite-dimensional) Navier-Stokes equation can be considered in the linear system framework discussed in Curtain and Zwart (1995). Among others, for the linearized Navier-Stokes equation, one can find stabilizing controllers based on finite inputs and outputs and investigate their robustness with the theory of coprime factorizations that is also well developed for infinite-dimensional linear systems; see (Curtain and Zwart, 1995, Ch. 9) and Vidyasagar (1985). In this work, we provide the theory for robust controller design under linearization uncertainties and numerical algorithms that compute the margins that guarantee stability.

This paper is structured as follows. In Section 2, we review standard theory on robust control and coprime

⋆ The first and third authors were supported by the German Research Foundation (DFG) priority program 1897: "Calm, Smooth and Smart – Novel Approaches for Influencing Vibrations by Means of Deliberately Introduced Dissipation" and the German Research Foundation (DFG) research training group 2297 "MathCoRe", Magdeburg.

2405-8963 © 2019, IFAC (International Federation of Automatic Control) Hosting by Elsevier Ltd. All rights reserved.
Peer review under responsibility of International Federation of Automatic Control.
10.1016/j.ifacol.2019.08.005

factorizations, and apply it to the case of linearization uncertainty. We formulate the relevant equations for finite element discretizations of the linearized incompressible Navier-Stokes equation in Section 3 and provide numerical results on the robustness margins of controllers for the 2D cylinder wake in Section 4. We conclude the paper by a summary and interpretation of the presented theory and results.

2. LINEARIZATION UNCERTAINTIES

In the considered setup, the transfer function of the (linearized, semi-discrete) Navier-Stokes equation with inputs and outputs is strictly proper; see Ahmad et al. (2017). This means it can be realized via ODEs as state equations, and the controller design and analysis can be done with standard ODE theory. For the numerical simulations, however, a realization as descriptor system is preferable; see Benner and Heiland (2015).

In the same vein, a finite-element model typically comes with a mass matrix. For the theory this matrix can be eliminated by a state-transformation or a scaling of the state equations. In practice, all algorithms are readily extended to efficiently accommodate such a matrix factor. Similarly, we assume that possible weighting parameters from the underlying *LQG* problem are resolved in state transforms or scaling of the inputs.

With these simplifications, in theory, a controller can be based on a standard linear time-invariant (LTI) system

$$\dot{x} = Ax + Bu, \tag{1a}$$
$$y = Cx, \tag{1b}$$

that represents a linearization of the nonlinear system about a steady-state.

If there is uncertainty in the linearization point, we have to assume that the exact linearization is of the form

$$\dot{x} = [A + A_\Delta]x + Bu, \tag{2a}$$
$$y = Cx, \tag{2b}$$

where A_Δ is the difference to the computed linearization.

Let $G\colon s \mapsto G(s) \in \mathbb{C}^{p\times m}$ and $G_\Delta\colon s \mapsto G_\Delta(s) \in \mathbb{C}^{p\times m}$ be the transfer functions associated with (1) and (2), respectively.

The question is now, whether a controller K, that was designed to stabilize G, does also stabilize the actual dynamics G_Δ. A quantitative answer to that is provided by the theory of $\mathcal{H}_\infty$-robust controllers and *coprime factorizations* of the transfer functions; see McFarlane and Glover (1990).

Let (M, N) be a left coprime factorization of $G = M^{-1}N$ and let $(M+M_\Delta, N+N_\Delta)$ be a left coprime factorization of $G_\Delta = (M+M_\Delta)^{-1}(N+N_\Delta)$. Here M, $M+M_\Delta \in R\mathcal{H}_\infty^{p\times p}$ and N, $N+N_\Delta \in R\mathcal{H}_\infty^{p\times m}$. Accordingly, as a difference of stable transfer functions, M_Δ and N_Δ are also stable.

If now a given controller K, stabilizing G, is such that

$$\left\| \begin{bmatrix} K \\ I_p \end{bmatrix} (I_p - GK)^{-1} M^{-1} \right\|_{\mathcal{H}_\infty} \leq \epsilon^{-1}, \tag{3}$$

then K also stabilizes G_Δ provided that the difference in the coprime factors $\Delta := [N_\Delta \;\; M_\Delta] \in R\mathcal{H}_\infty^{p\times(p+m)}$ is small, namely

$$\|\Delta\|_{\mathcal{H}_\infty} < \epsilon;$$

see (McFarlane and Glover, 1990, Cor. 3.7).

For our considerations, we will use the *central controller* K_0 that, for a suitable γ, can be defined via the stabilizing solutions X_∞, Y_∞ of the two normalized $\mathcal{H}_\infty$ Riccati equations

$$C^TC + A^TX + XA + X(\gamma^{-2}BB^T - BB^T)X = 0, \tag{4}$$
$$BB^T + AY + YA^T + Y(\gamma^{-2}C^TC - C^TC)Y = 0. \tag{5}$$

This *output-based* controller K_0 satisfies (3) with $\epsilon^{-1} = \gamma$; see (McFarlane and Glover, 1990, Ch. 4.3.2).

For convenience, we set $\beta := 1 - \gamma^{-2}$.

Moreover, with Y_∞ solving (5) and thus $A - \beta Y_\infty C^TC$ being stable, a left coprime factorization of $G = M^{-1}N$ is given via

$$[N \;\; M] = \left[\begin{array}{c|cc} A - \beta Y_\infty C^T C & B & -\beta Y_\infty C^T \\ \hline C & 0 & I \end{array}\right]; \tag{6}$$

see (Mustafa and Glover, 1991, Lem. 5.7).

If we assume that also $A + A_\Delta - \beta Y_\infty C^TC$ is stable, then

$$[\tilde{N} \;\; \tilde{M}] = \left[\begin{array}{c|cc} A + A_\Delta - \beta Y_\infty C^T C & B & -\beta Y_\infty C^T \\ \hline C & 0 & I \end{array}\right] \tag{7}$$

defines a left coprime factorization of G_Δ.

Remark 1. Note that, since $\beta Y_\infty C^TC$ in fact defines a state feedback, the claim of $A+A_\Delta-\beta Y_\infty C^TC$ being stable is a much weaker claim than $A + A_\Delta$ being stabilized by an output-based controller K. The existence of uniformly stabilizing state feedbacks could be observed in our numerical experiments and is in line with known robustness results; see, e.g., Doyle (1978).

In general, the modeling error A_Δ is not known. In our numerical tests on the linearization error, however, we can compute the difference in the coefficients and, with the solution of the $\mathcal{H}_\infty$ filter Riccati equation (5) and the constructions in (6) and (7), also the difference $\Delta = (\tilde{M} - M, \tilde{N} - N)$ in the coprime factors. The error $\|\Delta\|_{\mathcal{H}_\infty}$ is given as the $\mathcal{H}_\infty$ norm of the difference of the associated transfer functions, i.e., as the maximum singular value of

$$C(sI - A_{\Delta;LC})^{-1}B_{N|M} - C(sI - A_{LC})^{-1}B_{N|M} \tag{8}$$

taken over $s \in i\mathbb{R}$, where we have used the abbreviations

$$A_{LC} := A - \beta Y_\infty C^TC,$$
$$A_{\Delta;LC} := A + A_\Delta - \beta Y_\infty C^TC,$$
$$B_{N|M} := \begin{bmatrix} B & -\beta Y_\infty C^T \end{bmatrix}.$$

3. REALIZATION FOR INCOMPRESSIBLE FLOWS

The LTI system that is used for the controller design for a semi-discretized linearized incompressible Navier-Stokes equation reads

$$E\dot{v} = Av + J^Tp + Bu, \quad v(0) = v_0 \tag{9a}$$
$$0 = Jv, \tag{9b}$$

together with the output definition

$$y = Cv, \tag{9c}$$

where $v(t) \in \mathbb{R}^{n_v}$ approximates the velocity, $p(t) \in \mathbb{R}^{n_p}$ approximates the pressure, and where the mass matrix

$E \in \mathbb{R}^{n_v,n_v}$ is symmetric and invertible, as is $JE^{-1}J^T$. We define

$$\mathcal{E} = \begin{bmatrix} E & 0 \\ 0 & 0 \end{bmatrix}, \quad \text{and} \quad \mathcal{A} = \begin{bmatrix} A & J^T \\ J & 0 \end{bmatrix},$$

as well as

$$\mathcal{B} = \begin{bmatrix} B \\ 0 \end{bmatrix}, \quad \text{and} \quad \mathcal{C} = [C \ 0],$$

and write the (transfer function of) system (9) as

$$\left[\begin{array}{c|c} -s\mathcal{E} + \mathcal{A} & \mathcal{B} \\ \hline \mathcal{C} & 0 \end{array}\right] \quad \longleftrightarrow \quad G(s) = \mathcal{C}(s\mathcal{E} - \mathcal{A})^{-1}\mathcal{B}.$$

If the initial value v_0 is consistent, i.e., $Jv_0 = 0$, then system (9) can be equivalently realized via

$$\left[\begin{array}{c|c} -sE + \bar{A} & \bar{B} \\ \hline \bar{C} & 0 \end{array}\right], \tag{10}$$

where $\bar{A} := \Pi^T A \Pi$, $\bar{B} := \Pi^T B$, and $\bar{C} := C\Pi$, and where $\Pi := I_{n_v} - E^{-1}J^T(JE^{-1}J^T)^{-1}J$ is the discrete Leray projector; see, e.g., Ahmad et al. (2017) for an analysis of these transfer functions.

Remark 2. Due to the involvement of the projector Π, the matrices

$$\begin{bmatrix} \bar{A} - \lambda E & \bar{B} \end{bmatrix} \quad \text{and} \quad \begin{bmatrix} \bar{A} - \lambda E \\ \bar{C} \end{bmatrix}$$

are rank deficient for $\lambda = 0$ and, thus, the projected system is not stabilizable or detectable. However, since the state v evolves in the range of Π, those zeros that are associated with the kernel of Π can be eliminated from the theoretical consideration, e.g., by a factorization of Π as in Heinkenschloss et al. (2008). However, to avoid another change of variables and since the solutions of the Riccati equations employed for controller design are not affected by these components, we stick to the form (10) and understand stabilizability/detectability only with respect to the range of Π.

For the realization (10), the $\mathcal{H}_\infty$-Gramians can be obtained via $X_\infty = E\bar{X}_\infty E$ and $Y_\infty = \bar{Y}_\infty$, where $\bar{X}_\infty$ and $\bar{Y}_\infty$ are the unique stabilizing solutions of

$$\bar{C}^T\bar{C} + \bar{A}^T X E + E X \bar{A} - \beta E X \bar{B}\bar{B}^T X E = 0, \tag{11}$$

$$\bar{B}\bar{B}^T + \bar{A} Y E + E Y \bar{A}^T - \beta E Y \bar{C}^T\bar{C} Y E = 0. \tag{12}$$

We note that, like for standard Riccati equations, the solutions to (11) and (12) can be numerically computed without resorting to the projector Π; see, e.g., Bänsch et al. (2015).

In accordance to (6), with a stabilizing solution $\bar{Y}_\infty$, a left coprime factorizations of (10) is given by

$$[N \ M] = \left[\begin{array}{c|cc} E^{-1}\bar{A} - \beta\bar{Y}_\infty\bar{C}^T\bar{C} & E^{-1}\bar{B} & -\beta\bar{Y}_\infty\bar{C}^T \\ \hline \bar{C} & 0 & I \end{array}\right]. \tag{13}$$

Since we can assume that $\bar{Y}_\infty = \Pi\bar{Y}_\infty\Pi^T$ (Benner and Heiland, 2018, Rem. 5), we infer that

$$\begin{aligned} \bar{Y}_\infty\bar{C}^T &= \Pi\bar{Y}_\infty\Pi^T\bar{C}^T \\ &= \Pi E E^{-1}\bar{Y}_\infty\Pi^T\bar{C}^T \\ &= E^{-1}\Pi^T E\bar{Y}_\infty\bar{C}^T, \end{aligned}$$

such that (13) can be realized as

$$[N \ M] = \left[\begin{array}{c|cc} -s\mathcal{E} + \mathcal{A}_{LC} & \mathcal{B} & -\mathcal{L} \\ \hline \mathcal{C} & 0 & I \end{array}\right], \tag{14}$$

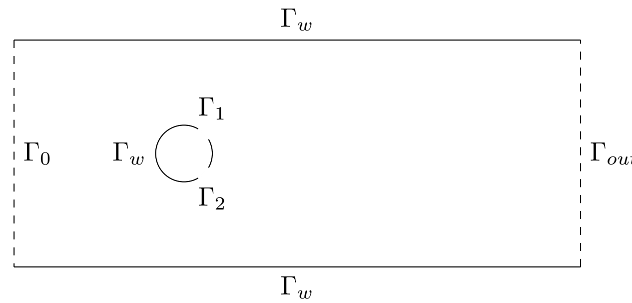

Fig. 1. Computational domain of the cylinder wake.

where

$$\mathcal{A}_{LC} := \begin{bmatrix} A - \beta E Y_\infty C^T C & J^T \\ J & 0 \end{bmatrix} \quad \text{and}$$

$$\mathcal{L} := \begin{bmatrix} \beta E Y_\infty C^T \\ 0 \end{bmatrix}.$$

The corresponding perturbed system can be realized in the same way without resorting to the projector Π. Thus, for a given perturbation A_Δ in the coefficient matrix A of the linearized incompressible Navier-Stokes equation (9), the perturbation in a left coprime factorization can be computed as in (8) via the $\mathcal{H}_\infty$ norm of the difference of transfer functions with realizations of the form (14).

4. NUMERICAL SETUP

We consider a Navier-Stokes equation that models the velocity v and the pressure p of an incompressible flow for the time $t > 0$ in a domain Ω with boundary $\Gamma = \Gamma_0 \cup \Gamma_w \cup \Gamma_{out} \cup \Gamma_1 \cup \Gamma_2$, as illustrated in Figure 1,

$$\dot{v} + (v \cdot \nabla)v + \nabla p - \nu\Delta v = 0, \quad \text{in } \Omega, \tag{15a}$$

$$\operatorname{div} v = 0, \quad \text{in } \Omega, \tag{15b}$$

with inflow and outflow boundary conditions

$$v = -ng_0 \cdot \alpha \text{ on } \Gamma_0 \quad \text{and} \quad \nu\frac{\partial v}{\partial n} - np = 0 \text{ on } \Gamma_{out}, \tag{15c}$$

and boundary control

$$v = -ng_1 \cdot u_1 \text{ on } \Gamma_1 \quad \text{and} \quad v = -ng_2 \cdot u_2 \text{ on } \Gamma_2, \tag{15d}$$

where ν is a diffusion parameter and n is the outward normal vector, g_0, g_1, and g_2 are shape functions modeling the spatial extension and where α, u_1, and u_2 control the magnitude and direction of the flow at the boundary, and with *no-slip* conditions at the walls, i.e., $v = 0$ on Γ_w.

The concrete setup is, as described in Behr et al. (2017), with the height of the channel $|\Gamma_0| = 0.41$ and the diameter of the cylinder $D = 0.1$. Notably, the Dirichlet boundary conditions (15d) are approximated by *Robin-type* boundary conditions (which then ensure that the operator that maps the controls into the dual of the state-space is bounded; see (Benner and Heiland, 2016, Sec. 3)) and the inflow profile g_0 is a parabola that is zero at the upper and the lower wall and scaled such that the average velocity satisfies $\frac{1}{|\Gamma_0|}\int_{\Gamma_0} g_0 \cdot \alpha ds = \alpha$. As is standard, we remove the physical dimensions of the equations by suitable scalings and parametrize them by means of the *Reynolds number* Re, which, in this setup, we define as $Re = \frac{\alpha \cdot D}{\nu}$ and which we have set to $Re = 100$ in the presented numerical examples.

Table 1. The difference in the linearization point, the difference in the coprime factorizations, and the robustness margin of the central controller for varying accuracy in the approximation v_ℓ of v_∞.

ℓ	$\frac{\|v_\infty - v_\ell\|_E}{\|v_\infty\|_E}$	$\|\Delta_\ell\|_{\mathcal{H}_\infty}$	γ_ℓ^{-1}
3	0.094	2.323	0.103
5	0.030	0.579	0.204
6	0.018	0.168	0.233
7	0.011	0.226	0.237
8	0.006	0.123	0.240
10	0.002	0.028	0.242

We discretize the domain by Taylor-Hood finite elements of order (2/1), which use P_2 finite elements for the discretization of the velocity state-space and P_1 for the pressure state-space. The constructed triangulation of the domain approximates the velocity with $n_v = 19\,500$ degrees of freedom. Thus, after linearization, the problem (15) is modeled by the linear system of differential-algebraic equations (DAEs)

$$E\dot{v} = Av + J^T p + Bu, \tag{16a}$$
$$0 = Jv, \tag{16b}$$

to which we add the linear observation operator C

$$y = Cv, \tag{16c}$$

as spatially averaged velocities measured downstream in the wake of the cylinder; see (Behr et al., 2017, Sec. 10.2) for a precise description. In the presented numerical tests, we considered 3 *sensor points* such that, because the velocities have two components, measurements result in $y(t) \in \mathbb{R}^6$.

If the linearization (16) was computed around a steady-state v_∞ of the corresponding nonlinear system, then a controller designed to stabilize (16) will also (locally) stabilize v_∞ in the actual nonlinear system; see Raymond (2006) for results for the infinite-dimensional Navier-Stokes equation.

We investigate the performance of controllers based on (16) linearized around a state v_ℓ that is not exactly the desired steady-state, but, as in this setup, the state that is reached by the Picard iteration employed to compute v_∞ starting from the corresponding *Stokes-solution* after ℓ steps.

Let A_ℓ and A_∞ be the coefficient matrices corresponding to the linearizations about v_ℓ and v_∞, respectively. Then, for given ℓ, with

$$A := A_\ell \quad \text{and} \quad A_{\Delta;\ell} := A_\infty - A_\ell,$$

we are in the setting described by (1) and (2). In fact, since J and E are not affected by the linearization error, the corresponding DAE systems of type (16) can be simultaneously realized as ODE systems, as explained in Section 3. However, for the computation of the $\mathcal{H}_\infty$-Gramians (11) and (12), as well as for the computation of the $\mathcal{H}_\infty$ norm of the coprime factor perturbations $\Delta_\ell := (\tilde{M} - M_\ell, \tilde{N} - N_\ell)$ via the transfer function defined in (8) we use the projector-free realizations like in (14).

In Table 1 we report the error in the coprime factors that is caused by an inaccurate linearization over $v_\ell \approx v_\infty$ and compare it to γ_ℓ^{-1}, where γ_ℓ is the robustness of the *central controller* K_ℓ, compare (3), computed on the base of the corresponding inaccurate linearization via the solutions of (4) and (5). In theory, the controller K_ℓ will stabilize the inexact linearization, whenever $\|\Delta_\ell\|_{\mathcal{H}_\infty} \leq \gamma_\ell^{-1}$, which we achieve for $\ell \geq 6$.

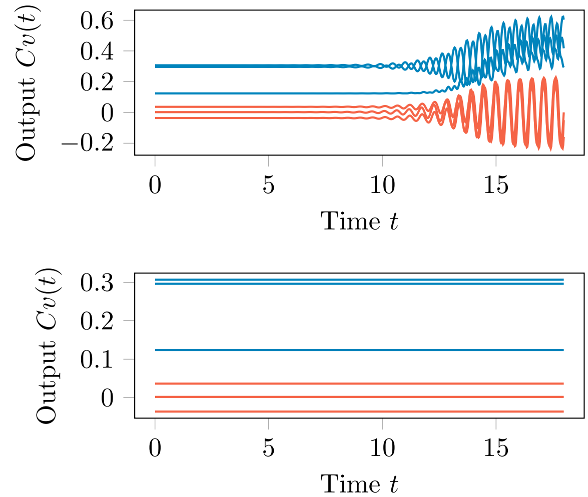

Fig. 2. The components of the output $y = Cv$ of the nonlinear Navier-Stokes system (15) after spatial discretization and if integrated from the steady state v_∞ that was slightly perturbed to trigger the instabilities. The upper plot shows the output measured in the uncontrolled case and the lower plot shows the output of the closed-loop system with the central controller K_8. In both plots, the blue lines correspond to the components in x direction and the red lines to the components in y direction.

We confirmed the stabilizing property of K_8 even for the nonlinear system in a numerical simulation as follows. The spatially discretized (nonlinear) Navier-Stokes equations (15) were numerically integrated in time using the semi-explicit trapezoidal rule and starting from $v_\infty + \delta$. Here, δ is a random perturbation with $\|\delta\|_E = 10^{-5}$ and $J\delta = 0$.

If no control is applied, the initial perturbation δ gets amplified and the system gradually enters a periodic regime known as vortex shedding. This can be clearly seen from the response shown in the upper plot of Figure 2. If, however, the loop is closed with the *central controller* K_8 that defines the control based on the current control error $Cv(t) - Cv_\infty$, then the system is kept close to the steady state v_∞; see the lower plot of Figure 2. Thus, although it was designed via a corrupted linearization, the controller K_8 is capable to compensate the initial and further perturbations due to the numerical error in the time discretization and the linearization.

5. CONCLUSION

As presented, the standard central robust $\mathcal{H}_\infty$-controller is capable to compensate model uncertainties that arise from linearization errors. The provided formulas to estimate the robustness were extended to cover the case of the incompressible Navier-Stokes equation with a strictly proper transfer function. The formulation in the discrete

(FEM) approximations of the operators allows for actual computation of the errors also in the large-scale setting. All results are in line with considerations of the infinite-dimensional model and serve as a base to design robust controllers for partial differential equations based on finite-dimensional approximations.

REFERENCES

Ahmad, M.I., Benner, P., Goyal, P., and Heiland, J. (2017). Moment-matching based model reduction for Navier-Stokes type quadratic-bilinear descriptor systems. *Z. Angew. Math. Mech.*, 97(10), 1252–1267. doi:10.1002/zamm.201500262.

Badra, M. (2006). *Stabilisation par Feedback et Approximation des Equations de Navier-Stokes*. Ph.D. thesis, Université Paul Sabatier, Toulouse.

Bänsch, E., Benner, P., Saak, J., and Weichelt, H.K. (2015). Riccati-based boundary feedback stabilization of incompressible Navier-Stokes flows. *SIAM J. Sci. Comput.*, 37(2), A832–A858. doi:10.1137/140980016.

Behr, M., Benner, P., and Heiland, J. (2017). Example setups of Navier-Stokes equations with control and observation: Spatial discretization and representation via linear-quadratic matrix coefficients. e-print arXiv:1707.08711, arXiv. URL `https://arxiv.org/abs/1707.08711`. Cs.MS, math.DS.

Benner, P. and Heiland, J. (2015). LQG-balanced truncation low-order controller for stabilization of laminar flows. In R. King (ed.), *Active Flow and Combustion Control 2014*, volume 127 of *Notes on Numerical Fluid Mechanics and Multidisciplinary Design*, 365–379. Springer International Publishing. doi:10.1007/978-3-319-11967-0_22.

Benner, P. and Heiland, J. (2016). Robust stabilization of laminar flows in varying flow regimes. *IFAC-PapersOnLine*, 49(8), 31–36. doi:10.1016/j.ifacol.2016.07.414. 2nd IFAC Workshop on Control of Systems Governed by Partial Differential Equations CPDE 2016, Bertinoro, Italy, 13–15 June 2016.

Benner, P. and Heiland, J. (2017). Convergence of approximations to Riccati-based boundary-feedback stabilization of laminar flows. *IFAC-PapersOnLine*, 50(1), 12296–12300. doi:10.1016/j.ifacol.2017.08.2476. 20th IFAC World Congress.

Benner, P. and Heiland, J. (2018). Exponential stability and stabilization of extended linearizations via continuous updates of Riccati based feedback. *Internat. J. Robust Nonlinear Control*, 28(4), 1218–1232. doi:10.1002/rnc.3949.

Curtain, R.F. and Zwart, H. (1995). *An Introduction to Infinite-Dimensional Linear Systems Theory*, volume 21 of *Texts in Applied Mathematics*. Springer-Verlag, New York. doi:10.1007/978-1-4612-4224-6.

Doyle, J. (1978). Guaranteed margins for LQG regulators. *IEEE Trans. Autom. Control*, 23(4), 756–757. doi:10.1109/TAC.1978.1101812.

Heinkenschloss, M., Sorensen, D.C., and Sun, K. (2008). Balanced truncation model reduction for a class of descriptor systems with application to the Oseen equations. *SIAM J. Sci. Comput.*, 30(2), 1038–1063. doi:10.1137/070681910.

McFarlane, D.C. and Glover, K. (1990). *Robust Controller Design Using Normalized Coprime Factor Plant Descriptions*, volume 138 of *Lecture Notes in Control and Inform. Sci.* Springer-Verlag, Berlin/Heidelberg. doi:10.1007/BFB0043199.

Morris, K.A. (1994). Convergence of controllers designed using state-space techniques. *IEEE Trans. Autom. Control*, 39(10), 2100–2104. doi:10.1109/9.328802.

Mustafa, D. and Glover, K. (1991). Controller reduction by $\mathcal{H}_\infty$-balanced truncation. *IEEE Trans. Autom. Control*, 36(6), 668–682. doi:10.1109/9.86941.

Raymond, J.P. (2006). Feedback boundary stabilization of the two-dimensional Navier-Stokes equations. *SIAM J. Control Optim.*, 45(3), 790–828. doi:10.1137/050628726.

Vidyasagar, M. (1985). *Control system synthesis: a factorization approach*. Signal Processing, Optimization, and Control. The MIT Press.